CLNS 97/1503, CLEO 97-19
CLEO CONF 97-12
EPS Abstract #338

Search for Color-Suppressed B Hadronic Decays Processes with CLEO

CLEO Collaboration

Abstract

Using 3.1 fb^{-1} of data accumulated at the Υ(4S) by the CLEO-II detector, corresponding to 3.3 million $B\bar{B}$ pairs, we have searched for the color-suppressed B hadronic decay processes: $\bar{B}^0 \to D^0(D^{*0})\mathrm{X}^0$, where X^0 is a light neutral meson π^0, ρ^0, η, $\eta^{'}$ or ω. The D^{*0} mesons are reconstructed in $D^{*0} \to D^0\pi^0$ and the D^0 mesons in $D^0 \to K^-\pi^+$, $K^-\pi^+\pi^0$ and $K^-\pi^+\pi^+\pi^-$ decay modes. No obvious signal is observed. We set 90% C.L. upper limits on these modes, varying from 1.2 $\times 10^{-4}$ for $\bar{B}^0 \to D^0\pi^0$ to 1.9 $\times 10^{-3}$ for $\bar{B}^0 \to D^{*0}\eta^{'}$.

(To be submitted to Physical Review D)

D. W. Bliss,[1] G. Masek,[1] H. P. Paar,[1] S. Prell,[1] V. Sharma,[1] D. M. Asner,[2] J. Gronberg,[2] T. S. Hill,[2] D. J. Lange,[2] S. Menary,[2] R. J. Morrison,[2] H. N. Nelson,[2] T. K. Nelson,[2] C. Qiao,[2] J. D. Richman,[2] D. Roberts,[2] A. Ryd,[2] M. S. Witherell,[2] R. Balest,[3] B. H. Behrens,[3] W. T. Ford,[3] H. Park,[3] J. Roy,[3] J. G. Smith,[3] J. P. Alexander,[4] C. Bebek,[4] B. E. Berger,[4] K. Berkelman,[4] K. Bloom,[4] D. G. Cassel,[4] H. A. Cho,[4] D. S. Crowcroft,[4] M. Dickson,[4] P. S. Drell,[4] K. M. Ecklund,[4] R. Ehrlich,[4] A. D. Foland,[4] P. Gaidarev,[4] L. Gibbons,[4] B. Gittelman,[4] S. W. Gray,[4] D. L. Hartill,[4] B. K. Heltsley,[4] P. I. Hopman,[4] J. Kandaswamy,[4] P. C. Kim,[4] D. L. Kreinick,[4] T. Lee,[4] Y. Liu,[4] G. S. Ludwig,[4] N. B. Mistry,[4] C. R. Ng,[4] E. Nordberg,[4] M. Ogg,[4,1] J. R. Patterson,[4] D. Peterson,[4] D. Riley,[4] A. Soffer,[4] B. Valant-Spaight,[4] C. Ward,[4] M. Athanas,[5] P. Avery,[5] C. D. Jones,[5] M. Lohner,[5] C. Prescott,[5] J. Yelton,[5] J. Zheng,[5] G. Brandenburg,[6] R. A. Briere,[6] A. Ershov,[6] Y. S. Gao,[6] D. Y.-J. Kim,[6] R. Wilson,[6] H. Yamamoto,[6] T. E. Browder,[7] Y. Li,[7] J. L. Rodriguez,[7] T. Bergfeld,[8] B. I. Eisenstein,[8] J. Ernst,[8] G. E. Gladding,[8] G. D. Gollin,[8] R. M. Hans,[8] E. Johnson,[8] I. Karliner,[8] M. A. Marsh,[8] M. Palmer,[8] M. Selen,[8] J. J. Thaler,[8] K. W. Edwards,[9] A. Bellerive,[10] R. Janicek,[10] D. B. MacFarlane,[10] P. M. Patel,[10] A. J. Sadoff,[11] R. Ammar,[12] P. Baringer,[12] A. Bean,[12] D. Besson,[12] D. Coppage,[12] C. Darling,[12] R. Davis,[12] N. Hancock,[12] S. Kotov,[12] I. Kravchenko,[12] N. Kwak,[12] S. Anderson,[13] Y. Kubota,[13] S. J. Lee,[13] J. J. O'Neill,[13] S. Patton,[13] R. Poling,[13] T. Riehle,[13] V. Savinov,[13] A. Smith,[13] M. S. Alam,[14] S. B. Athar,[14] Z. Ling,[14] A. H. Mahmood,[14] H. Severini,[14] S. Timm,[14] F. Wappler,[14] A. Anastassov,[15] J. E. Duboscq,[15] D. Fujino,[15,2] K. K. Gan,[15] T. Hart,[15] K. Honscheid,[15] H. Kagan,[15] R. Kass,[15] J. Lee,[15] M. B. Spencer,[15] M. Sung,[15] A. Undrus,[15,3] R. Wanke,[15] A. Wolf,[15] M. M. Zoeller,[15] B. Nemati,[16] S. J. Richichi,[16] W. R. Ross,[16] P. Skubic,[16] M. Bishai,[17] J. Fast,[17] J. W. Hinson,[17] N. Menon,[17] D. H. Miller,[17] E. I. Shibata,[17] I. P. J. Shipsey,[17] M. Yurko,[17] S. Glenn,[18] S. D. Johnson,[18] Y. Kwon,[18,4] S. Roberts,[18] E. H. Thorndike,[18] C. P. Jessop,[19] K. Lingel,[19] H. Marsiske,[19] M. L. Perl,[19] D. Ugolini,[19] R. Wang,[19] X. Zhou,[19] T. E. Coan,[20] V. Fadeyev,[20] I. Korolkov,[20] Y. Maravin,[20] I. Narsky,[20] V. Shelkov,[20] J. Staeck,[20] R. Stroynowski,[20] I. Volobouev,[20] J. Ye,[20] M. Artuso,[21] A. Efimov,[21] M. Goldberg,[21] D. He,[21] S. Kopp,[21] G. C. Moneti,[21] R. Mountain,[21] S. Schuh,[21] T. Skwarnicki,[21] S. Stone,[21] G. Viehhauser,[21] X. Xing,[21] J. Bartelt,[22] S. E. Csorna,[22] V. Jain,[22,5] K. W. McLean,[22] S. Marka,[22] R. Godang,[23] K. Kinoshita,[23] I. C. Lai,[23] P. Pomianowski,[23] S. Schrenk,[23] G. Bonvicini,[24] D. Cinabro,[24] R. Greene,[24] L. P. Perera,[24] G. J. Zhou,[24] B. Barish,[25] M. Chadha,[25] S. Chan,[25] G. Eigen,[25] J. S. Miller,[25] C. O'Grady,[25] M. Schmidtler,[25] J. Urheim,[25] A. J. Weinstein,[25] and F. Würthwein[25]

[1]University of California, San Diego, La Jolla, California 92093
[2]University of California, Santa Barbara, California 93106
[3]University of Colorado, Boulder, Colorado 80309-0390
[4]Cornell University, Ithaca, New York 14853
[5]University of Florida, Gainesville, Florida 32611
[6]Harvard University, Cambridge, Massachusetts 02138
[7]University of Hawaii at Manoa, Honolulu, Hawaii 96822

[1]Permanent address: University of Texas, Austin TX 78712
[2]Permanent address: Lawrence Livermore National Laboratory, Livermore, CA 94551.
[3]Permanent address: BINP, RU-630090 Novosibirsk, Russia.
[4]Permanent address: Yonsei University, Seoul 120-749, Korea.
[5]Permanent address: Brookhaven National Laboratory, Upton, NY 11973.

[8]University of Illinois, Champaign-Urbana, Illinois 61801
[9]Carleton University, Ottawa, Ontario, Canada K1S 5B6
and the Institute of Particle Physics, Canada
[10]McGill University, Montréal, Québec, Canada H3A 2T8
and the Institute of Particle Physics, Canada
[11]Ithaca College, Ithaca, New York 14850
[12]University of Kansas, Lawrence, Kansas 66045
[13]University of Minnesota, Minneapolis, Minnesota 55455
[14]State University of New York at Albany, Albany, New York 12222
[15]Ohio State University, Columbus, Ohio 43210
[16]University of Oklahoma, Norman, Oklahoma 73019
[17]Purdue University, West Lafayette, Indiana 47907
[18]University of Rochester, Rochester, New York 14627
[19]Stanford Linear Accelerator Center, Stanford University, Stanford, California 94309
[20]Southern Methodist University, Dallas, Texas 75275
[21]Syracuse University, Syracuse, New York 13244
[22]Vanderbilt University, Nashville, Tennessee 37235
[23]Virginia Polytechnic Institute and State University, Blacksburg, Virginia 24061
[24]Wayne State University, Detroit, Michigan 48202
[25]California Institute of Technology, Pasadena, California 91125

I. INTRODUCTION

The B hadronic decays $\bar{B}^0 \to D^0(D^{*0})\mathrm{X}^0$, where X^0 is a light neutral meson π^0, ρ^0, η, $\eta^{'}$ or ω, have not yet been observed. These decays proceed via the internal spectator diagram shown in Figure 1. The internal spectator decays are expected to be suppressed relative to the decays that proceed via

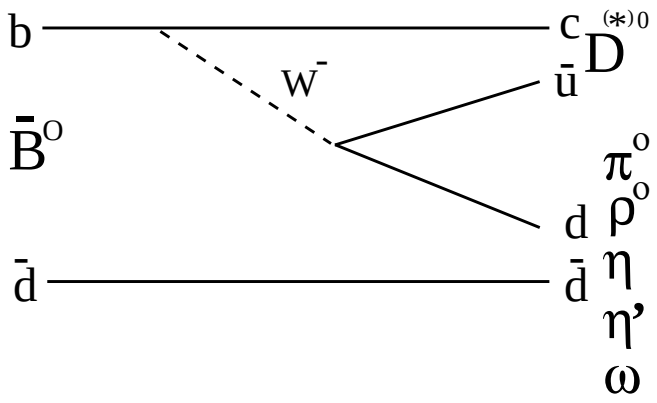

Figure 1: Internal spectator diagram of B hadronic decays $\bar{B}^0 \to D^0(D^{*0})\mathrm{X}^0$.

external spectator diagrams, since the color of the quarks from the virtual W must match the color of the c quark and the accompanying spectator antiquark. Therefore these decays are refered to as color-suppressed decays, while decays via external spectator diagrams are refered to as color-favored decays. Measurements of these color-suppressed decays allow tests of the factorization [1] hypothesis and provide useful information on the scale of strong final-state interaction in the B meson system.

Previous CLEO papers [2] reported upper limits on these color-suppressed B hadronic decays. Here we present new results using the full CLEO-II data set and an improved analysis method.

II. DATA SAMPLE and EVENT SELECTION

The data used in this analysis were produced in e^+e^- annihilations at the Cornell Electron Storage Ring (CESR) and collected with the CLEO-II detector [3]. The intergrated luminosity is 3.1 fb^{-1} at the Υ(4S) resonance, which corresponds to (3.32$\pm$0.07) $\times$ 10^6 $B\bar{B}$ pairs, and 1.6 fb^{-1} at energies just below $B\bar{B}$ threshold (henceforth referred to as the continuum).

Hadronic events are selected by requiring at least three charged tracks, a total detected energy of at least 0.15 $\mathrm{E}_{c.m}$, and a primary vertex within 5.0 cm along the beam (z) axis of the interaction point. To suppress continuum background, we require that the ratio of second to zeroth Fox-Wolfram moments R_2 [4] determined using charged tracks and unmatched neutral showers be less than 0.3 (0.5 for clean decay modes involving η or $\eta^{'}$). To further reduce continuum background, we then require that the cosine of the angle between the sphericity axis of the B meson candidate and the sphericity axis of the remainder of the event satisfies $|\cos(\theta_{sphericity})| < 0.8$ (0.9 for decay modes involving η or $\eta^{'}$). For a jet-like continuum event, the two axes are almost parallel, while they are almost uncorrelated for a $B\bar{B}$ event,

III. B RECONSTRUCTION

Selection of D^0 and D^{*0} candidates

The D^0 candidates are reconstructed in the decay modes $D^0 \to K^-\pi^+$, $K^-\pi^+\pi^0$ and $K^-\pi^+\pi^+\pi^-$ (charge-conjugate modes are implied). The π^0 candidates are formed by combining two showers whose invariant mass is within 2.5σ of the π^0 mass (where henceforth σ denotes r.m.s. resolution). Charged tracks are required to be consistent with coming from the interaction region in both the $r-\phi$ and $r-z$ planes. The measured specific inoization (dE/dx) of charged kaon and pion candidates are required to be consistent to within 2σ for kaon candidates and 3σ for pion candidates. Charged tracks are required to have a momentum greater than 250 MeV for $D^0 \to K^-\pi^+$ and $D^0 \to K^-\pi^+\pi^0$ candidates and 200 MeV for $D^0 \to K^-\pi^+\pi^+\pi^-$ candidates. For $D^0 \to K^-\pi^+\pi^0$ decay mode, we select regions of the Dalitz plot with large amplitude to further suppress the combinatoric backgrounds. The invariant mass of D^0 candidates is required to be within 2.0σ of the nominal D^0 mass.

The D^{*0} candidates are reconstructed using decay mode $D^{*0} \to D^0\pi^0$. We form D^{*0} candidates by D^0 candidates using above selection, then require that the $D^{*0} - D^0$ mass difference be within 2.5σ of the measured value [5].

Selection of the light neutral meson X^0

We reconstruct π^0 candidates as described previously. The ρ^0 candidates are reconstructed in the mode $\rho^0 \to \pi^+\pi^-$.

Candidate η and η' mesons are reconstructed in their $\eta \to \gamma\gamma$ and $\eta' \to \eta\pi^+\pi^-$ decay modes. The absolute value of the η decay angle is required to be less than 0.85 to remove asymmetric candidates which are primarily background. The invariant mass of each η and η' candidate must be within 30 MeV of their nominal mass.

The ω mesons are reconstructed in the decay mode $\omega \to \pi^+\pi^-\pi^0$. Charged and neutral pions are required to have momenta greater than 250 MeV, to reject soft pions from D^{*0} or D^{*+} decays. The ω candidates are also required to be within 30 MeV of the nominal ω mass.

All charged pion candidates used in X^0 reconstruction are required to have a measured dE/dx within 3σ of the expected value for pions.

Selection of the B candidates

The $D^{(*)0}$ candidates are combined with a light X^0 to form a B meson. At CLEO the energy of the B meson is the same as the beam energy and the measured beam energy is more precise than the reconstructed B meson energy. Full reconstruction of B mesons at CLEO makes use of this fact by defining two variables. One is the beam-constrained mass, $\mathrm{M}_B \equiv \sqrt{E^2_{beam} - P^2_{observed}}$. The other one is the difference between the reconstructed energy and the beam energy, $\Delta E \equiv E_{observed} - E_{beam}$. The ΔE variable is sensitive to missing or extra particles in the B decay, as well as particle species. For fully-reconstructed B meson decays, the M_B distribution peaks at 5.28 GeV with resolution around 2.7 MeV, and ΔE peaks at 0.0 GeV with a resolution ranging from 18 to 50 MeV, depending on the B and D^0 decay modes.

Since signal and background are in general much better seperated in ΔE than in M_B, instead of cutting on the ΔE variable and fitting M_B as in previous analyses, we cut on M_B and fit the ΔE distribution for the signal yield.

IV. BACKGROUND STUDY

In our search for the color-suppressed B hadronic decay modes $\bar{B}^0 \to D^{(*)0}(\pi^0, \rho^0, \eta, \eta', \omega)$, there are backgrounds to these decays from continuum and $B\bar{B}$ events. The continuum backgrounds are suppressed using event-shape variables. They are not expected to show any structure in the ΔE distributions. The 1.6 fb^{-1} continuum data set is used to monitor the continuum background levels. We find the continuum background level to be very low for all color-suppressed modes. No accumulation around $\Delta E = 0$ is observed in the continuum data.

The backgrounds from $B\bar{B}$ events are dominated by feedthrough from color-favored two-body hadronic decays of the type:

$$B^- \to D^0(\pi^-, \rho^-, a_1^-),\ B^- \to D^{*0}(\pi^-, \rho^-, a_1^-)$$
$$\bar{B}^0 \to D^+(\pi^-, \rho^-, a_1^-),\ \bar{B}^0 \to D^{*+}(\pi^-, \rho^-, a_1^-)$$

The branching ratios of these color-favored B meson decay modes were measured previously by CLEO [2]. In most cases the background arises when a real, energetic D^0 or D^{*0} from the 2-body color-favored decays is combined with a fake light meson.

The backgrounds from these color-favored processes can have structure in the M_B and ΔE distributions, depending on which color-suppressed mode is being analyzed. Particularly important are color-favored B meson decays that give exactly the same final state particles as our color-suppressed signals do. Neither misidentification nor additional particles are needed for those color-favored decays to fake some signal modes. Therefore, the M_B distribution from these physics background peaks at 5.28 GeV while its ΔE distribution peaks at 0.0 GeV, exactly as the color-suppressed signal. While $D^0\pi^0$ is not susceptible to this background $D^0\rho^0$ and $D^0\omega$ are, as shown below.

Color – favored :	$\bar{B}^0 \to D^{*+}\pi^- \to D^0\pi^+\pi^-$	$\bar{B}^0 \to D^{*+}\rho^- \to D^0\pi^+\pi^-\pi^0$
Color – suppressed :	$\bar{B}^0 \to D^0\rho^0 \to D^0\pi^+\pi^-$	$\bar{B}^0 \to D^0\omega \to D^0\pi^+\pi^-\pi^0$

Another background that can show structure is color-favored decay in which one of the final state particles is lost. Examples include:

Color – favored :	$\bar{B}^0 \to D^0\pi^0$	$\bar{B}^0 \to D^0\rho^0 \to D^0\pi^+\pi^-$
Color – suppressed :	$B^- \to D^0\rho^- \to D^0\pi^0\ (\pi^-)$	$\bar{B}^0 \to D^{*+}\rho^- \to D^0\pi^+\pi^-\ (\pi^0)$

These background events can peak in M_B around 5.28 GeV when the missing π^- or π^0 from the ρ^- decay is very soft and does not contribute much to the beam-constrained mass calculation. However, the ΔE for these background events differs from zero by more than one pion mass, due to the missing π^- or π^0 from the ρ^- decay. For these types of color-favored backgrounds, the color-suppressed signals are much better separated from background in ΔE.

For decay modes involving η or η', combinatoric background is the dominating source. Therefore, backgrounds for these color-suppressed processes have no accumulation in the M_B and ΔE distributions.

For $\bar{B}^0 \to D^{*0}X^0$, there is no corresponding color-favored B meson decay that fakes our signal as $\bar{B}^0 \to D^{*+}\pi^-$ fakes $\bar{B}^0 \to D^0\rho^0$. Also the background level from color-favored B meson decays is very low for $\bar{B}^0 \to D^{*0}X^0$ decay processes, due to the good resolution on the $D^{*0} - D^0$ mass difference.

Almost all the discrimination power against color-favored physics backgrounds come from selection cuts on X^0. We make full use of mass, momentum, decay angle and other kinematic variables of X^0 to suppress backgrounds while keeping signal efficiency as high as possible.

The X^0 candidates in $\bar{B}^0 \to D^{(*)0}X^0$ tend to be very energetic due to the hard spectrum of two-body B meson decays. We require the momentum of the π^0 candidate to range from 2.1 GeV to 2.5 GeV. Similar momentum requirements are imposed on the other light neutral meson X^0 candidates.

For $\bar{B}^0 \to D^0\rho^0$ decays, there are color-favored physics backgrounds from $\bar{B}^0 \to D^{*+}\pi^-$ that give exactly the same final state particles. The $B^- \to D^0\rho^-$ decay can also fake our color-suppressed signal by substituting the soft π^0 from ρ^- decay by a soft π^+ from the other B meson. In these physics backgrounds, the π^- is always much more energetic than the π^+ from $D^{*+} \to D^0\pi^+$ decay. There exists a correlation between the D^0 and the fast π^- (slow π^+) from the fake ρ^0. To suppress these physics backgrounds, we require that the D^0 candidate to be associated with a fast π^+ (slow π^-) from the ρ^0 candidate. There is still a contribution from color-favored physics backgrounds even after this requirement, because a D^0 decay has a certain chance of being misidentified as a $\bar{D}^0$ decay. For the D^0's from our signal process, together with the dE/dx and D^0 mass requirements, this misidentification rate is determined to be less than 20%. After further suppression due to the ρ^0 mass and momentum requirements, the contribution from color-favored physics background is negligible. Since the ρ^0 from $\bar{B}^0 \to D^0\rho^0$ decay is longitudinally polarized, we also cut on the ρ^0 decay angle (the angle between the direction of the pion in the ρ^0 rest frame and the direction of the ρ^0 in the lab frame) to reduce combinatoric backgrounds.

Signal selection efficiencies for all the color-suppressed decay modes are shown in Table 1. The systematic error due to the detection of charged and neutral tracks, together with the Monte Carlo statistical error, are included in the error on the efficiency for each decay mode.

Table 1: Selection efficiencies and yields of all color-suppressed modes. The three efficiencies and yields of each $\bar{B}^0 \to D^0(D^{*0})\mathrm{X}^0$ correspond to the three $D^0 \to K^-\pi^+$, $K^-\pi^+\pi^0$ and $K^-\pi^+\pi^+\pi^-$ modes.

Decay Mode	Selection Efficiency	Yield
$B^0 \to D^0\pi^0$	26.1±2.2, 7.8±1.0, 12.5±1.3%	-0.3±6.4, -6.7±4.3, -3.3±7.0
$\bar{B}^0 \to D^{*0}\pi^0$	14.1±1.8, 3.7±0.7, 5.4±0.9%	2.5±2.6, 5.0 ±3.4, -1.2±3.4
$B^0 \to D^0\rho^0$	8.4±0.4, 2.6±0.3, 3.9±0.3%	1.4±3.0, -3.0±4.3, 3.1±5.0
$B^0 \to D^{*0}\rho^0$	4.0±0.4, 1.0±0.2, 1.5±0.2%	-1.0±1.4, 1.4±1.6, 0.8±1.3
$B^0 \to D^0\eta$	24.5±3.0, 7.0±1.2, 11.4±1.6%	-1.4±2.0, -3.1±3.1, -6.0±4.0
$B^0 \to D^{*0}\eta$	10.5±1.8, 3.4±0.8, 4.9±0.9%	0, 0, 0
$\bar{B}^0 \to D^0\eta'$	13.4±1.9, 3.6±0.7, 5.9±1.0%	0, 0.8±2.2, 1.8±3.0
$\bar{B}^0 \to D^{*0}\eta'$	5.9±1.1, 1.7±0.4, 2.5±0.5%	0, 0, 1
$B^0 \to D^0\omega$	12.4±1.3, 2.8,±0.4, 3.2±0.5%	-4.1±4.0, 6.2±3.8, 3.6±5.6
$\bar{B}^0 \to D^{*0}\omega$	4.8±0.7, 1.0±0.2, 1.3±0.2%	1.8±1.2, 0.8 ±1.8, -0.2±1.2

V. RESULTS

The ΔE distributions for the on $\Upsilon(4S)$ and continuum data samples of all the color-suppressed signal processes after all cuts are shown in Fig. $2-6$. The ΔE distribution of each color-suppressed mode is fit with a Gaussian and a background shape function. The mean value and width of the Gaussian distribution are fixed with values determined from signal Monte Carlo. We use various color-favored decay modes $B^- \to D^0\pi^-$, $B^- \to D^0\rho^-$, $B^- \to D^{*0}\pi^-$, $B^- \to D^{*0}\rho^-$, $\bar{B}^0 \to D^+\pi^-$, $\bar{B}^0 \to D^+\rho^-$ to check that the ΔE resolutions in data and Monte Carlo agree well. Possible differences between data and Monte Carlo in the ΔE distributions are considered and included in the yield error as systematic errors.

Various ΔE background shape functions have been used to fit for the signal yield: a simple second-order polynomial; or a background shape using Monte Carlo simulation $B\bar{B}$ events plus a continuum component represented by a second-order polynomial. For the latter shape, the $B\bar{B}$ contribution is scaled to the known luminosity while the continuum component is allowed to float. Our results are found to be insensitive to different background shapes, and both of them describe the ΔE distributions reasonably well. Differences in the yield due to the choice of ΔE background shape are included in the yield error to account for the systematic uncertainties. For each signal process with several D^0 decay submodes, the yield for each D^0 submode is obtained seperately, since the ΔE resolutions are different for the different modes. The results are shown in Table 1. The yields of the D^0 submodes are added independently to get the total yield.

The formulas used to calculate the branching fractions are:

$$Br(\bar{B}^0 \to D^0 X^0) = \frac{N_{obs}}{N_{B\bar{B}} \times (\sum_{i=1}^{3} \text{Efficiency}(i) \times Br(D^0{}_i)) \times \prod Br(X^0)} \tag{1}$$

$$Br(\bar{B}^0 \to D^{*0} X^0) = \frac{N_{obs}}{N_{B\bar{B}} \times Br(D^{*0} \to D^0\pi^0) \times (\sum_{i=1}^{3} \text{Efficiency}(i) \times Br(D^0{}_i)) \times \prod Br(X^0)} \tag{2}$$

where N_{obs} is the total yield summed over the three D^0 submodes, $N_{B\bar{B}}$ is the number of $B\bar{B}$ pairs, Efficiency(i) is the selection efficiency for $\bar{B}^0 \to D^0(D^{*0})X^0$ decay in the ith D^0 submode, $Br(D^0{}_i)$ is the branching ratio of the ith D^0 decay mode, and $\prod Br(X^0)$ is the product over all the relevant branching fractions of the X^0 decay chain. Particle Data Group values for D^0, D^{*0}, η, η' and ω branching ratios are used in the upper limits calculation [5] and are listed in Table 2.

Table 2: Particle Data Group branching ratios that are used in the upper limit calculation for color-suppressed B hadronic decays.

Decay Mode	PDG Branching Ratio
$D^0 \to K^-\pi^+$	4.01±0.14%
$D^0 \to K^-\pi^+\pi^0$	13.8±1.0%
$D^0 \to K^-\pi^+\pi^+\pi^-$	8.1±0.5%
$D^{*0} \to D^0\pi^0$	63.6±2.8%
$\rho^0 \to \pi^+\pi^-$	100%
$\eta \to \gamma\gamma$	38.8±0.5%
$\eta' \to \eta\pi^+\pi^-$	43.7±1.5%
$\omega \to \pi^+\pi^-\pi^0$	88.8±0.7%

The upper limits of color-suppressed branching ratios are determined by the method described in section 17 of the Particle Data Group [5]. 90% C.L. upper limits on branching ratios of color-suppressed B hadronic decay processes, together with theoretical predictions [6], are shown in Table 3. Among all the decay modes, the upper limit for the $\bar{B}^0 \to D^0\pi^0$ mode is the lowest at 1.2×10^{-4}. All the upper limits on branching ratios are still higher than theoretical predictions [6, 7]. Compared with factorization and QCD based calculations, no dramatic enhancement of color-suppressed B hadronic decay branching ratios is observed, indicating that there is no sign of large scale final-state interaction in these B meson decay modes.

Table 3: 90% C.L. upper limits in branching ratios of all color-suppressed modes, together with comparison with theoretical predictions.

Decay Mode	Branching Ratio (@90% C.L.)	Theoretical Predictions
$\bar{B}^0 \to D^0\pi^0$	$< 1.2\times10^{-4}$	0.7×10^{-4}
$B^0 \to D^{*0}\pi^0$	$< 4.4\times10^{-4}$	1.0×10^{-4}
$\bar{B}^0 \to D^0\rho^0$	$< 3.9\times10^{-4}$	0.7×10^{-4}
$B^0 \to D^{*0}\rho^0$	$< 5.6\times10^{-4}$	1.7×10^{-4}
$\bar{B}^0 \to D^0\eta$	$< 1.3\times10^{-4}$	0.5×10^{-4}
$\bar{B}^0 \to D^{*0}\eta$	$< 2.6\times10^{-4}$	0.6×10^{-4}
$\bar{B}^0 \to D^0\eta^{'}$	$< 9.4\times10^{-4}$	
$\bar{B}^0 \to D^{*0}\eta^{'}$	$< 19\times10^{-4}$	
$B^0 \to D^0\omega$	$< 5.1\times10^{-4}$	0.7×10^{-4}
$\bar{B}^0 \to D^{*0}\omega$	$< 7.4\times10^{-4}$	1.7×10^{-4}

ACKNOWLEDGEMENTS

We gratefully acknowledge the effort of the CESR staff in providing us with excellent luminosity and running conditions. J.P.A., J.R.P., and I.P.J.S. thank the NYI program of the NSF, M.S. thanks the PFF program of the NSF, G.E. thanks the Heisenberg Foundation, K.K.G., M.S., H.N.N., T.S., and H.Y. thank the OJI program of DOE, J.R.P., K.H., M.S. and V.S. thank the A.P. Sloan Foundation, R.W. thanks the Alexander von Humboldt Stiftung, and M.S. thanks Research Corporation for support. This work was supported by the National Science Foundation, the U.S. Department of Energy, and the Natural Sciences and Engineering Research Council of Canada.

References

[1] J. Bjorken, Nucl. Phys. B (Proc. Suppl) **11** (1989) 325

[2] CLEO Collaboration, M.S. Alam *et al.*, Phys. Rev. D. **50** (1994) 43.

J.L. Rodriguez, Ph.D. Thesis, University of Florida (1995)

[3] CLEO Collaboration, Y. Kubota *et al.*, Nucl. Instrum. Methods A **320** (1992) 66.

[4] G. Fox and S. Wolfram, Phys. Rev. Lett. **23** (1992) 1581.

[5] Particle Data Group, Phys. Rev. D. **50** (1994) 1173.

[6] M. Neubert, V. Rieckert, B. Stech and Q.P. Xu in *Heavy Flavours*, edited by A. J. Buras and H. Lindner, World Scientific, Singapore (1992).

M. Neubert, B. Stech, HEP-PH/9705292

[7] A. Deandrea, N. Di Bartolomeo, R. Gatto and G. Nardulli, Phys. Lett. **B 318** (1993) 549

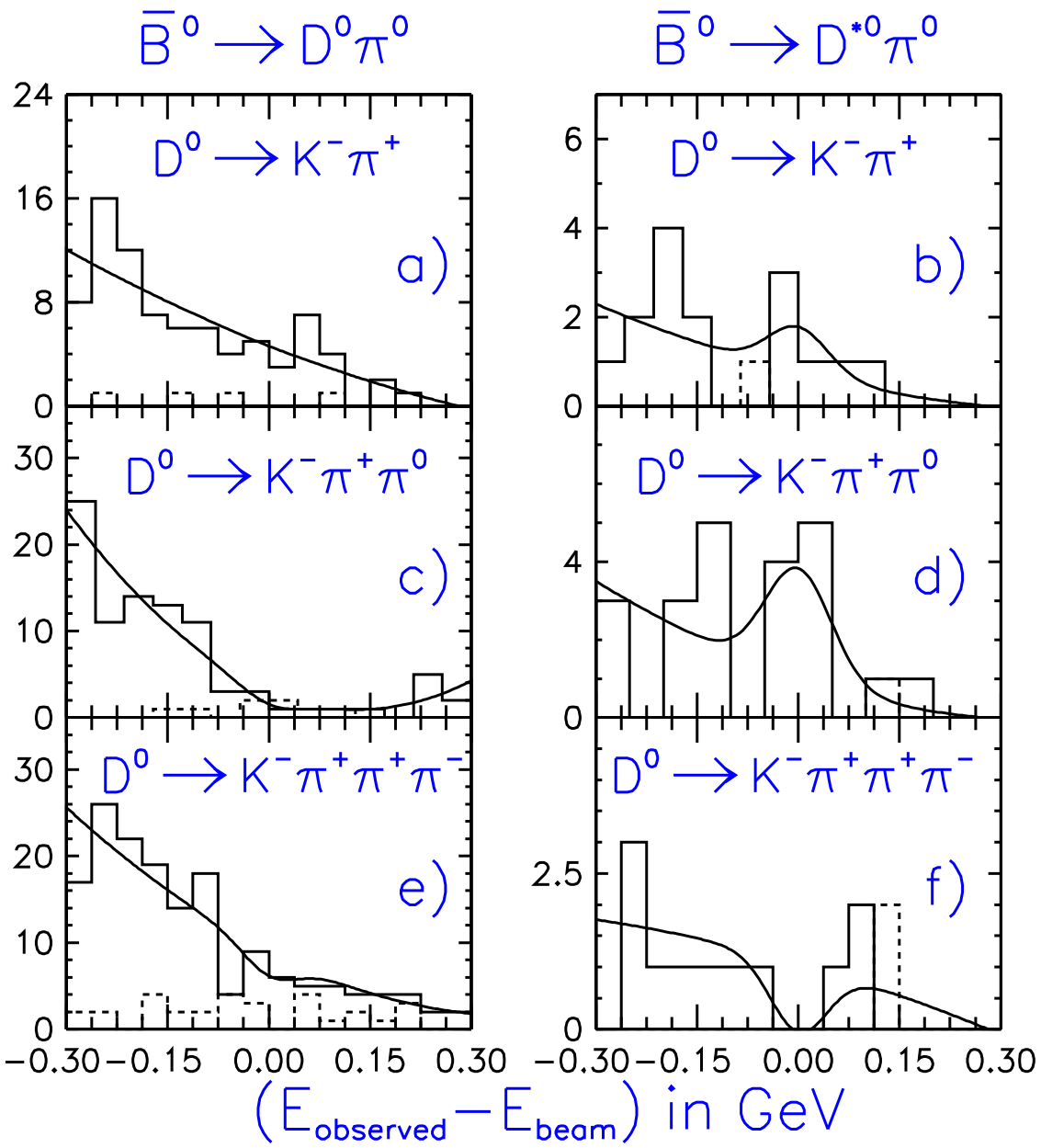

Figure 2: ΔE distributions of $\bar{B}^0 \to D^0\pi^0$ and $\bar{B}^0 \to D^{*0}\pi^0$ decay modes. Solid histograms are the ΔE distributions of the 3.1 fb^{-1} of data collected on the $\Upsilon(4S)$ resonance, which are fit using background and signal functions. Dashed histograms are from the 1.6 fb^{-1} continuum data sample.

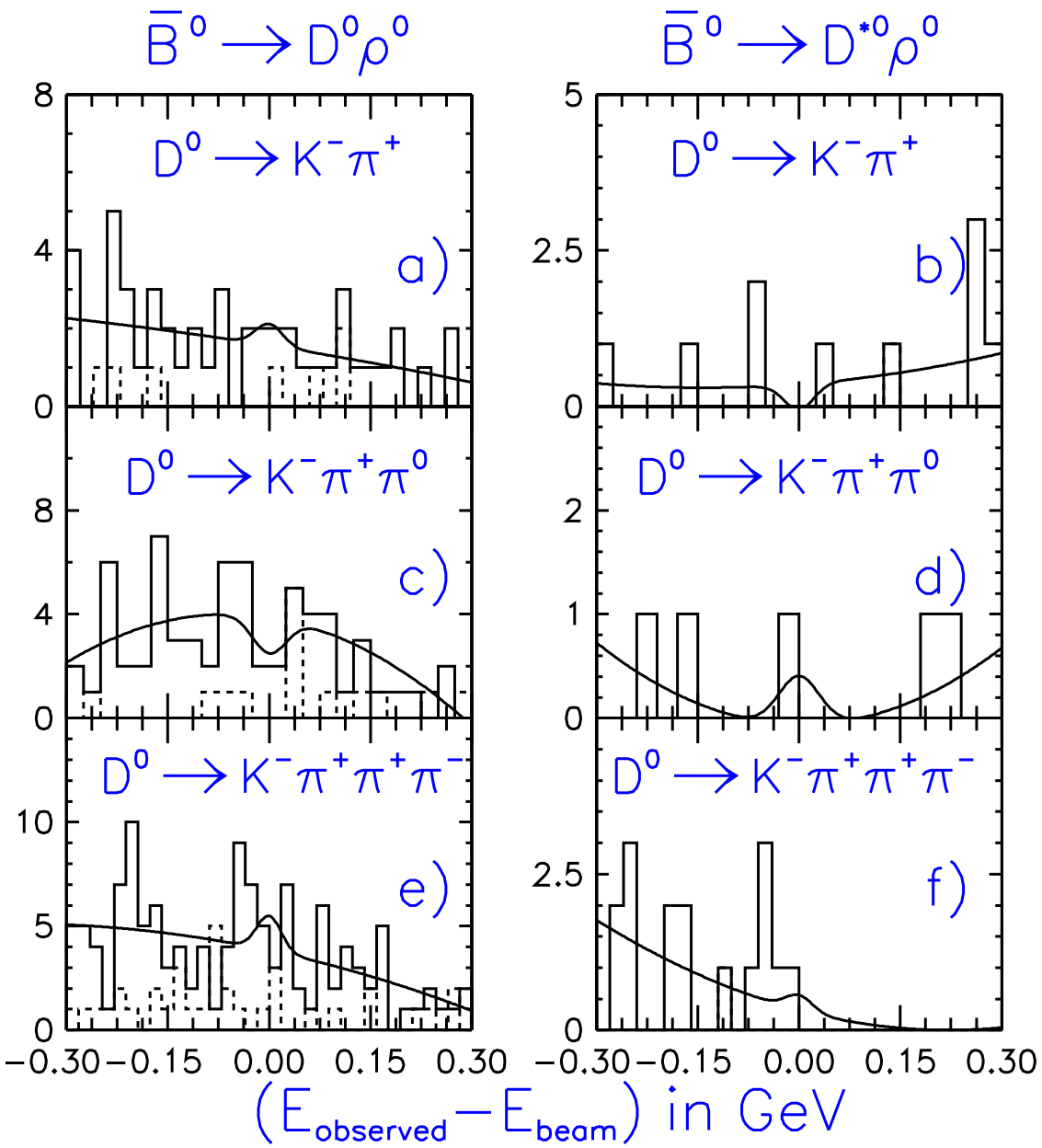

Figure 3: ΔE distributions of $\bar{B}^0 \to D^0\rho^0$ and $\bar{B}^0 \to D^{*0}\rho^0$ decay modes. Solid histograms are the ΔE distributions of the 3.1 fb^{-1} of data collected on the Υ(4S) resonance, which are fit using background and signal functions. Dashed histograms are from the 1.6 fb^{-1} continuum data sample.

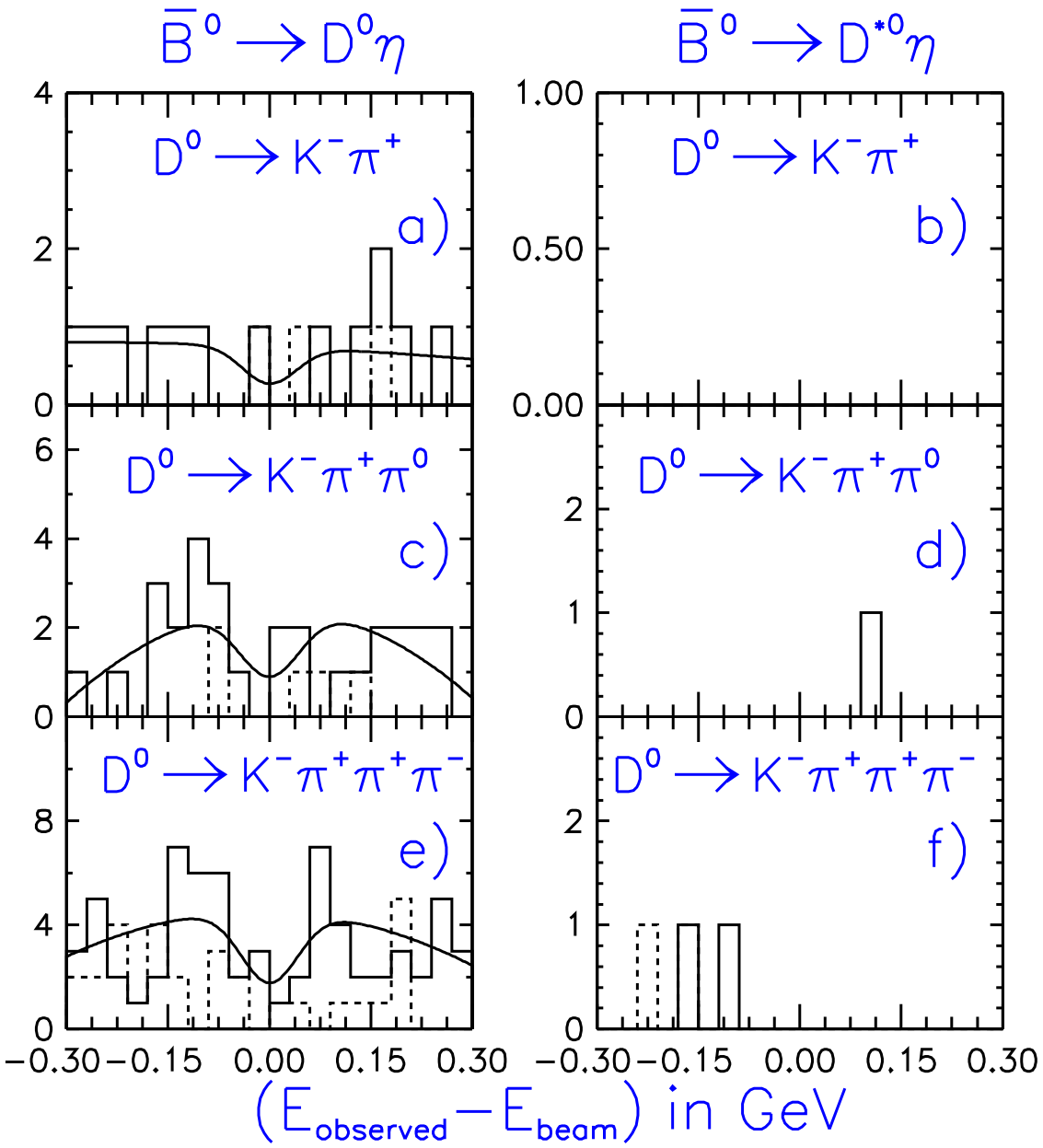

Figure 4: ΔE distributions of $\bar{B}^0 \to D^0\eta$ and $\bar{B}^0 \to D^{*0}\eta$ decay modes. Solid histograms are the ΔE distributions of the 3.1 fb^{-1} of data collected on the Υ(4S) resonance, which are fit using background and signal functions. Dashed histograms are from the 1.6 fb^{-1} continuum data sample.

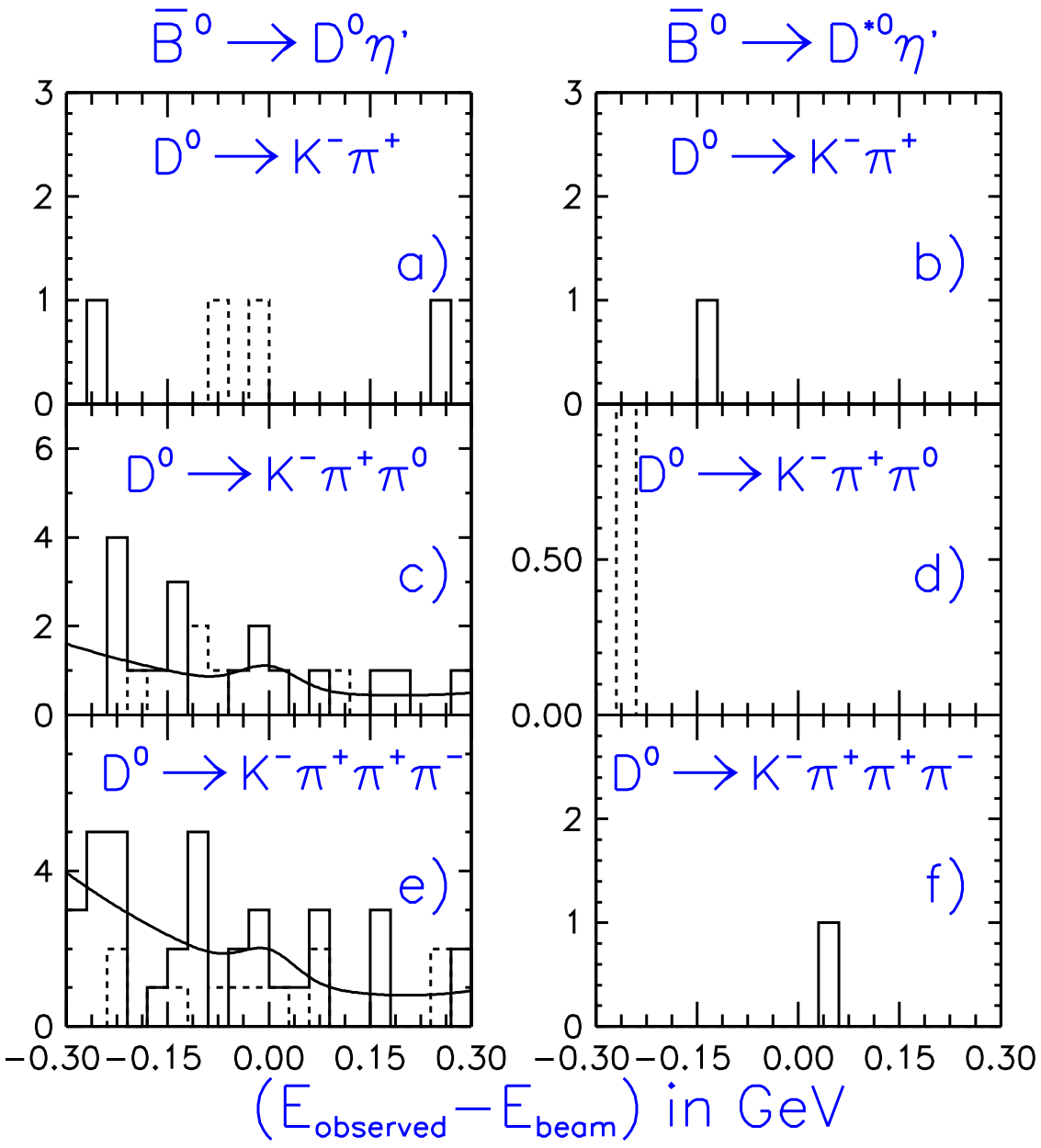

Figure 5: ΔE distributions of $\bar{B}^0 \to D^0\eta'$ and $\bar{B}^0 \to D^{*0}\eta'$ decay modes. Solid histograms are the ΔE distributions of the 3.1 fb^{-1} of data collected on the Υ(4S) resonance, which are fit using background and signal functions. Dashed histograms are from the 1.6 fb^{-1} continuum data sample.

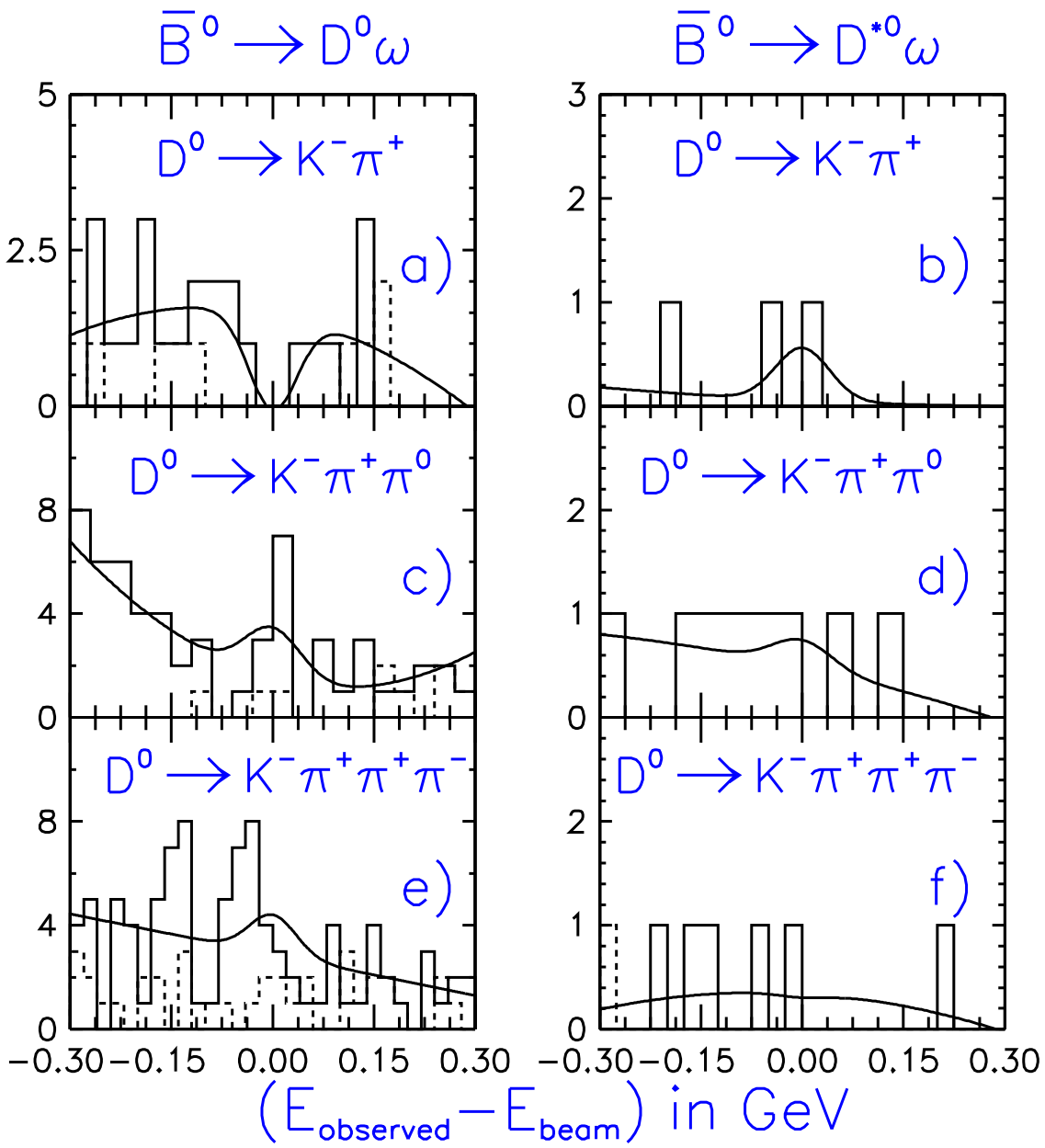

Figure 6: ΔE distributions of $\bar{B}^0 \to D^0\omega$ and $\bar{B}^0 \to D^{*0}\omega$ decay modes. Solid histograms are the ΔE distributions of the 3.1 fb^{-1} of data collected on the $\Upsilon(4S)$ resonance, which are fit using background and signal functions. Dashed histograms are from the 1.6 fb^{-1} continuum data sample.